Industrial Engineering Journal
ISSN: 0970-2555
Volume : 53, Issue 12, No.2, December : 2024

REGULATION OF FREQUENCY AND VOLTAGE IN SEIG FOR DISTRIBUTED GENERATION SYSTEM

Mr. Lingappa J, Research Scholar, Department of Electrical Engineering, University College of Engineering, Osmania University, Hyderabad, Telangana, India. E-mail: lingappa.ou@gmail.com
Sr. Prof. G. Yesuratnam, Professor, Department of Electrical Engineering, University College of Engineering, Osmania University, Hyderabad, Telangana India.
Dr. P. Mallikarjuna Sharma, Professor, Department of Electrical Engineering, Vasavi College of Engineering, Hyderabad, Telangana India

ABSTRACT
A phase locked loop (PLL) based control strategy for voltage source converters that does not make use of a voltage-controlled oscillator (VCO) is covered in this study. The control approach does not require a VCO because it applies a 3-phase to αβ transformation to obtain the fundamental extraction component from measured load current signal. In comparison to conventional synchronous reference frame (SRF) PLL, which necessitate a VCO and several transformations for basic extraction, the suggested approach greatly lessens the computing load related to trigonometric applications. A distributed generating system using wind power and having a self-excited induction generator (SEIG) installed that can serve as a linear and nonlinear load under various electrical conditions is the subject of the study. In addition to compensating for active and reactive power, the suggested control technique efficiently regulates the voltage and frequency constant. It also addresses neutral current.

Keywords:
VCO-Free PLL, SEIG, Voltage Source Inverter(VSI), Wind energy and Star-Delta(Y-Δ) transformer.

I. Introduction
Non-conventional energy generation has become a leading method of energy production in the 21st century [1]. The combustion of fossil fuels has contributed to major issues such as the greenhouse effect, increased pollution, and rising global temperatures. To safeguard future generations, it is crucial to enhance our reliance on alternative energy sources, including wind, solar, tidal, etc.[2]. Advances in technology have significantly mitigated the investment risks associated with these renewable sources. Among them, wind and solar energy are the most popular options for distributed generation systems. Advancements in the development of electric generators are making wind energy more feasible for both grid-connected and standalone systems [3]. Induction generators are particularly favored in wind energy applications because their simplicity, efficiency, and cost-effectiveness. The use of effective control techniques enhances the reliability of frequency and voltage in these systems [4]. S Golestan[5] has presented various types of phase-locked loops (PLL), which are used for measuring phase and frequency. These techniques play a crucial role in synchronization of grid and in regulating and measuring state variables. One of the limitations of PLLs is that the phase angle error exhibits both double-frequency ripple and an offset. Nevertheless, these methods are effective for grid synchronization, particularly when frequency and phase angle variations are slow. Additionally, this type of control can improve the load characteristics of generators, enabling the effective operation of shunt-connected power electronics devices like distributed static compensator (D-STATCOM) [5-8]. Various techniques can be used to synchronize power electronic converters through point of common interface (PCI) voltage, with PLL-based methods being the traditional and widely adopted [9-10]. However, synchronous reference frame PLLs (SRF-PLLs) has a significant drawback: they rely heavily on the quality of the input supply [11]. However, this approach faces two significant issues: slow transient performance, since the loop filter incorporates a moving average filter (MAF), and unable to generate unit templates. To address those challenges, a PLL having a high-performance VCO

Industrial Engineering Journal
ISSN: 0970-2555
Volume : 53, Issue 12, No.2, December : 2024

is proposed [12]. This VCO maintains fixed amplitude covariance at the estimated frequency but can become unstable because of two roots on the imaginary axis. Despite this, the signal amplitude remains stable due to integrator saturation, making the computation of trigonometric functions more manageable. The authors of this study have chosen to improve power quality in distribution systems by using VCO-free PLL approach. [13]. The primary objective of this control method is its ability to estimate amplitude, frequency, and unit vectors without relying on trigonometric calculations. While enhanced PLLs (EPLLs)[14-16] offer benefits, their reliance on the amplitude of the load current and the need for estimation of phase during fundamental extraction gives VCO-free PLLs an advantage, as they do not require phase-angle estimation. This approach significantly reduces the need for trigonometric calculations, resulting in a quicker performance with varying load.

In this paper, PLL without VCO control is employed to manage the voltage source converter (VSC)[17-21], enabling complete control of voltage and frequency across all operating ranges. This control mechanism is especially well-suited for applications with fast variations, like wind-based distributed generation, because it does not require a VCO. The control chosen for fundamental current extraction for three key reasons:

It doesn't require any complicated calculations involving trigonometric functions.

It operates with a smaller number of linear circuit components.

It has the ability to quickly track frequency, phase, and amplitude

II. System Description

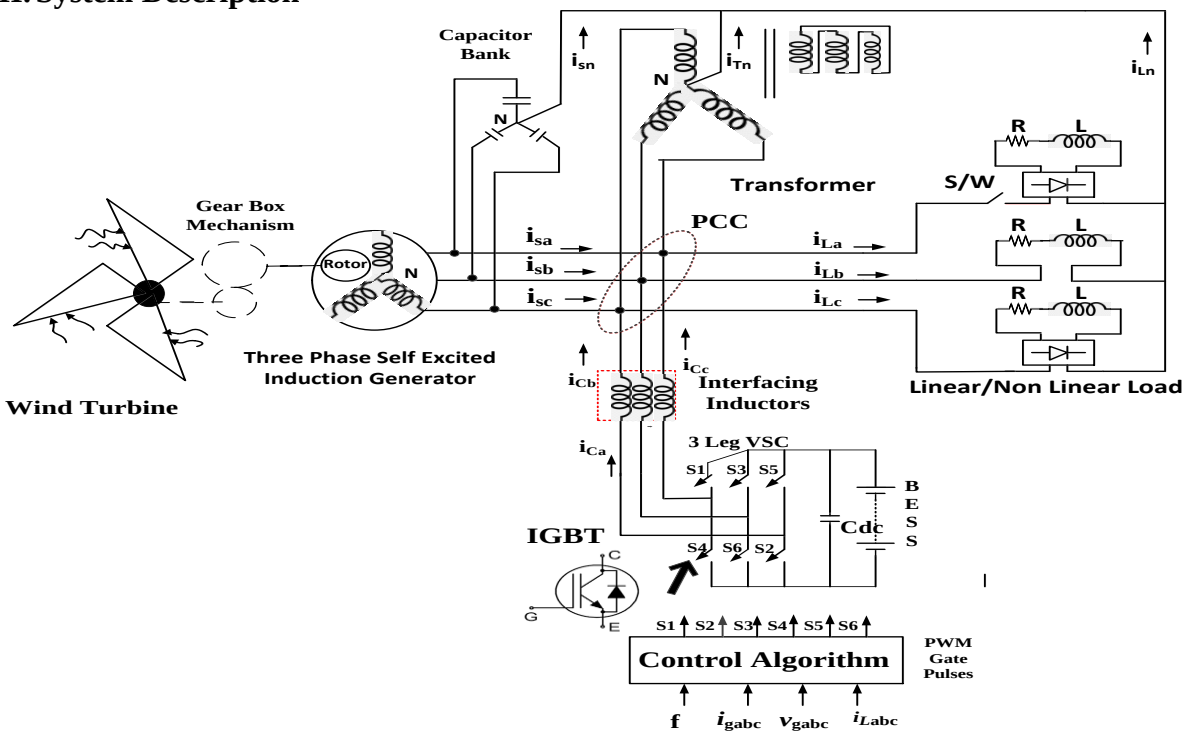

Figure 1: Proposed System Topology

Figure 1 shows the three-phase four wire (3P4W) system topology employed in this investigation. Key parts of the system include a wind turbine, a 3-phase self-excited induction generator (SEIG), three single-phase load units, a star-delta transformer, and a VSC that is connected to a battery energy storage system. For the induction generator to be able to self-excite, excitation capacitors are necessary. In addition to supporting the generator with reactive power, these capacitors also lessen noise caused by the high switching frequency of the VSI. Additionally, interfacing inductors for the three units are incorporated into the configuration, with their values determined by current ripple and switching frequency. The equipment is designed with appropriate rating considerations, with the turbine acting as the mechanical input for the induction generator. In isolated mode, the generator

Industrial Engineering Journal
ISSN: 0970-2555
Volume : 53, Issue 12, No.2, December : 2024

powers the three single-phase linear and nonlinear loads, which may be located remotely. These loads can sometimes become unbalanced, leading to current flow through the neutral wire. To mitigate this, a *Y-Δ* transformer is connected to neutralize the current in the fourth wire caused by load imbalance [6, 7]. The VSI consists six insulated gate bipolar transistors (IGBTs), arranged in a bridge configuration with three legs connected back-to-back.

III. Control Strategy

The control technique is employed for regulating the frequency and voltage of SEIG.

3.1 VCO-Free PLL

Figure 2 shows structural difference between SRF-PLL and VCO-Free PLL.This control estimating frequency, amplitude, and phase. A detailed mathematical model, represented by the transfer function, is also provided [13].

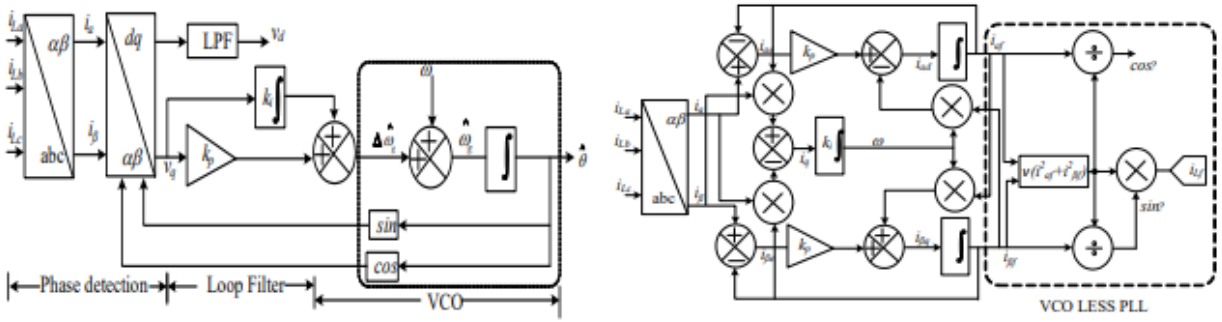

Figure 2: Structural difference between (a) SRF-PLL and (b) VCO-Less PLL

A) Frequency

$$\frac{di_\alpha}{dt} = -wi_\beta + k_p[i_\alpha - i_{\alpha f}] \tag{1}$$

$$\frac{di_\beta}{dt} = wi_\alpha + k_p[i_\beta - i_{\beta f}] \tag{2}$$

$$\frac{dw}{dt} = k_i i_q \tag{3}$$

Where, $i_q = i_\beta i_{\alpha f} - i_\alpha i_{\beta f}$

$$\frac{d^2w}{dt^2} = k_i \frac{di_q}{dt}$$

$$= k_i \left[\frac{di_\beta}{dt} i_{\alpha f} + i_\beta \frac{di_{\alpha f}}{dt} - i_{\beta f} \frac{di_{\alpha f}}{dt} - i_\alpha \frac{di_{\beta f}}{dt} \right] \tag{4}$$

$$= k_i(w_g - w)i_d - k_p \frac{dw}{dt}$$

Where, $i_d = i_\alpha i_{\alpha f} + i_\beta i_{\beta f}$ .Under the quasi -locked state, $i_d \cong I^2$

Consider $w = w_n + \Delta w$ and $w_g = w_n + \Delta w$ (2) can be written as

$$\Delta \frac{d^2w}{dt^2} = k_i(\Delta w_g - \Delta w)I^2 - k_p \frac{dw}{dt} \tag{5}$$

Applying Laplace transform of (5) gives

$$\frac{\Delta w(s)}{\Delta w_g(s)} = \frac{I^2 k_i}{s^2 + k_p s + I^2 k_i} \tag{6}$$

Industrial Engineering Journal
ISSN: 0970-2555
Volume : 53, Issue 12, No.2, December : 2024

Where, k_p and k_i are control parameters of (6).

B) Amplitude

Using Fig.2 (b), the amplitude measured by the VCO-free PLL can be expressed as

$$I = \sqrt{i_{\alpha f}^2 + i_{\beta f}^2} \tag{7}$$

Differentiating (7) with respect to time results in

$$\frac{dI}{dt} = \frac{\left[i_{\alpha f}\left(\frac{di_{\alpha f}}{dt}\right) + i_{\beta f}\left(\frac{di_{\beta f}}{dt}\right)\right]}{I} \tag{8}$$

Substituting equations (1) and (2) in equation (8) gives

$$\frac{dI}{dt} = k_p \frac{\left[i_\alpha - i_{\alpha f}\right] i_{\alpha f} + \left[i_\beta - i_{\beta f}\right] i_{\beta f}}{I}$$

$$= k_p \frac{\left(i_d - I^2\right)}{I}$$

$$\approx k_p \left(I - I^{\wedge}\right) \tag{9}$$

Applying Laplace transform to the above equation (9) is

$$\hat{I}(s) = \frac{k_p}{s + k_p} I(s) \tag{10}$$

C) Phase

It can be estimated as

$$\overset{\wedge}{\theta} = \tan^{-1}\left(\frac{\hat{i}_\beta}{\hat{i}_\alpha}\right) \tag{11}$$

Transfer function

$$\frac{\Delta \overset{\wedge}{\theta}(s)}{\Delta \theta(s)} = \frac{Ik_p s + Ik_i}{s^2 + Ik_p s + Ik_i} \tag{12}$$

Table -1 Comparison of VCO-Free PLL and conventional SRF-PLL

S.No	Parameters	VCO-Free PLL	SRF-PLL
1	Number of circuit components	Clarke transformation with adder, integrator and multiplier	Clarkes and parks transformation with phase detection, loop filter and VCO
2	Model type	Linear	Nonlinear (due to the presence of sine)
3	Computational burden	Very less	More (due to trigonometric calculations

3.2 Reference Current Generation

Figure 3 shows the block diagram of VCO-Free PLL for gate pulse generation. Terminal voltage (V_t) of three-phase source voltage is as follows

$$V_t = 0.812\left(v_{ga}^2 + v_{gb}^2 + v_{gc}^2\right) \tag{13}$$

Industrial Engineering Journal
ISSN: 0970-2555
Volume : 53, Issue 12, No.2, December : 2024

Where v_{ga},v_{gb} and v_{gc} are 3-phase instantaneous voltages. The unit template voltages are calculated is as follows,

$$u_{pa} = \frac{v_{ga}}{V_t}, u_{pb} = \frac{v_{gb}}{V_t}, u_{pc} = \frac{v_{gc}}{V_t} \quad (14)$$

$$\begin{pmatrix} u_{qa} \\ u_{qb} \\ u_{qc} \end{pmatrix} = \begin{pmatrix} \frac{1}{\sqrt{3}} & 0 & \frac{1}{\sqrt{3}} \\ \frac{\sqrt{3}}{2} & \frac{1}{\sqrt{3}} & -\frac{1}{\sqrt{3}} \\ \frac{\sqrt{3}}{2} & \frac{1}{2\sqrt{3}} & -\frac{1}{2\sqrt{3}} \end{pmatrix} \begin{pmatrix} u_{pa} \\ u_{pb} \\ u_{pc} \end{pmatrix} \quad (15)$$

Where (u_{pa},u_{pb},u_{pc}) and (u_{qa},u_{qb},u_{qc}) are the d-axis ad q-axis unit voltage templates of all the phase voltages.

To determine its instantaneous value, the amplitude of the fundamental load current (i_{Lf}) is extracted and then multiplied by the in-phase unit template. The fundamental load current's active and reactive components are identified using distinct sample-and-hold (S/H) circuits and zero-crossing detectors (ZCD). The first S/H circuit (S/H-1), which receives the instantaneous fundamental load current, gets edge-trigger pulses produced by applying quadrature-phase unit templates to its input (ZCD-1). The true output of S/H-1 is filtered using a low-pass filter (LPF) to determine the active component of the load current (i_{Lfd}). The second S/H circuit (S/H-2) is triggered by applying in-phase unit templates to the second ZCD (ZCD-2) in a parallel path to determine the reactive component (i_{Lfq}).

The d-axis of the reference current is expressed as below [6, 7]

$$i_{Ld} = i_{pa} - i_{Lfa}$$

$$i^*_{Ld} = i_{Ld} X u_{pabc} \quad (16)$$

The q-axis of the reference current is expressed as

$$i_{Lq} = i_q - i_{Lfq}$$

$$i^*_{Lq} = i_{Lq} X u_{qabc} \quad (17)$$

Therefore reference currents generation are computed by the following equation (18)

$$i^*_{gabc} = i^*_{Ld} + i^*_{Lq} \quad (18)$$

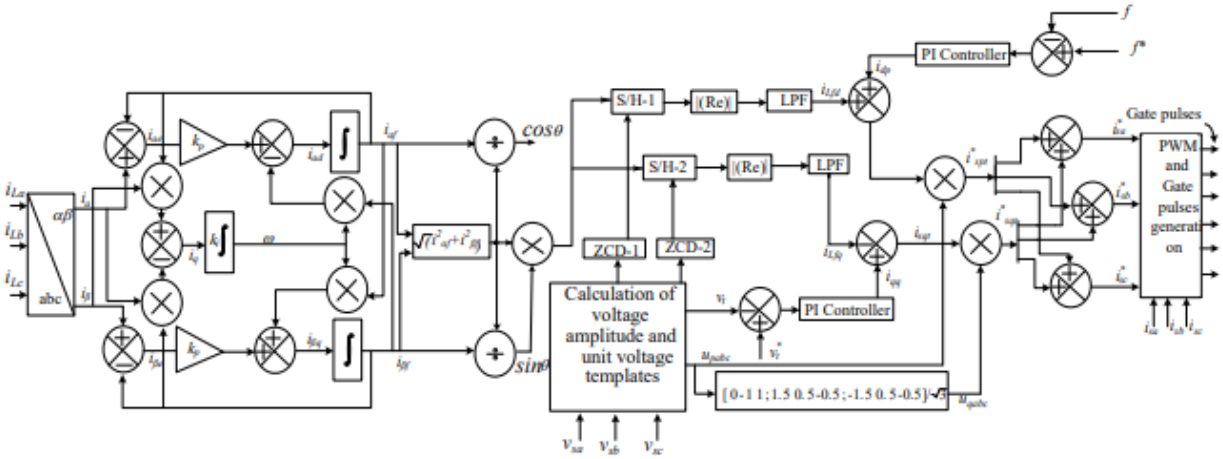

Figure 3: Block diagram of VCO-Free PLL for Gate pulse generation

1V Results and Discussion

Industrial Engineering Journal
ISSN: 0970-2555
Volume : 53, Issue 12, No.2, December : 2024

The study was conducted under both fixed and variable wind speed, along with varying load. The impact of the control algorithm on system performance was examined, focusing on regulation of frequency and voltage in SEIG within the system was observed.

4.1 Operation of SEIG at No-Load and Load

When there is no load, the transient response of SEIG and voltage buildup is shown in Figure 4. The AC capacitor bank is linked across the stator terminal of SEIG and provides reactive power assistance for the voltage buildup of SEIG. The bank of excitation capacitors has a voltage value that allows SEIG to reach its rated voltage of 400V (peak) when there is no load.

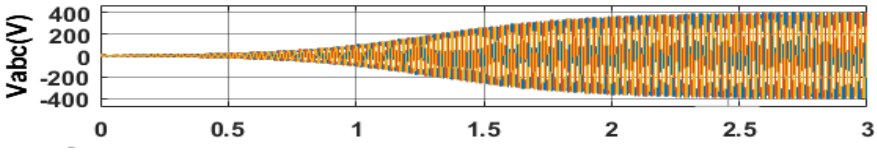

Figure 4: SEIG on No-Load

A balanced linear and non- linear load of 7Ω and 100mH is applied at t=2.5 sec, the generator voltage and capacitor current collapse as shown in Figure 5.

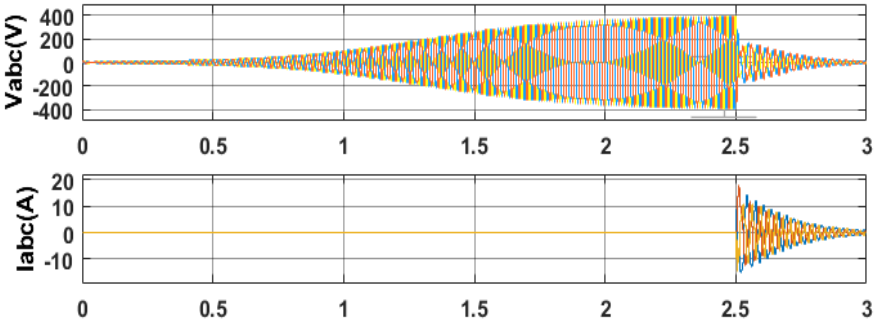

Figure 5: SEIG on Load

4.2 Transient response of SEIG with constant wind speed and variable nonlinear load

These parameters were measured: powers of generator, load and battery (P_g,Pl,Pb), frequency (f), wind speed (W_s), neutral current of transformer, load and supply (i_{Tn}, i_{Ln}, i_{Sn}), three-phase instantaneous voltage (V_{abc}) at the PCI, currents of generator, load and compensator (I_{abc}, I_{abcL}, I_{cabc}), terminal voltage amplitude (V_t), and more. The system is operating in steady state with a constant wind speed of 14 m/s from time t=2.5 seconds until time t=3.0 seconds. As seen in Figure 6, a transient happens at t=2.7 seconds when phase 'a' on the load side is disconnected, resulting in an unbalanced load. Because of the inherent imbalance, a tiny neutral current flowed in the load neutral during the steady state. Nevertheless, a notable rise in the load-side neutral current is noted upon disconnecting one phase. The delivering current in precise phase opposition to the load neutral current, the *Y-Δ* transformer and VSI make up for this imbalance.

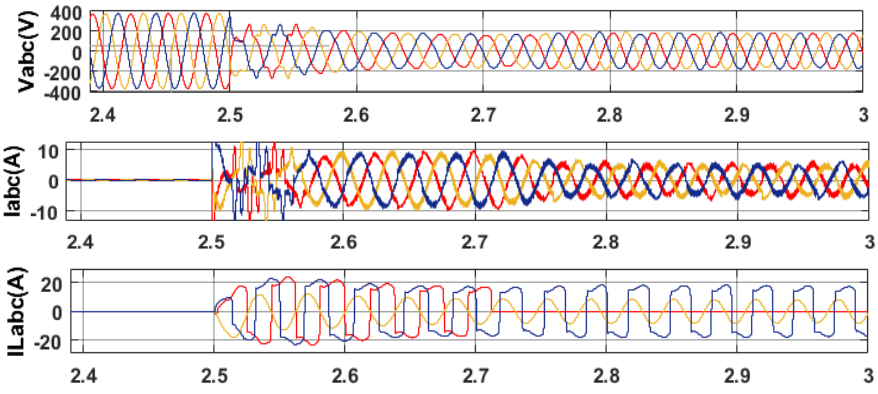

Industrial Engineering Journal
ISSN: 0970-2555
Volume : 53, Issue 12, No.2, December : 2024

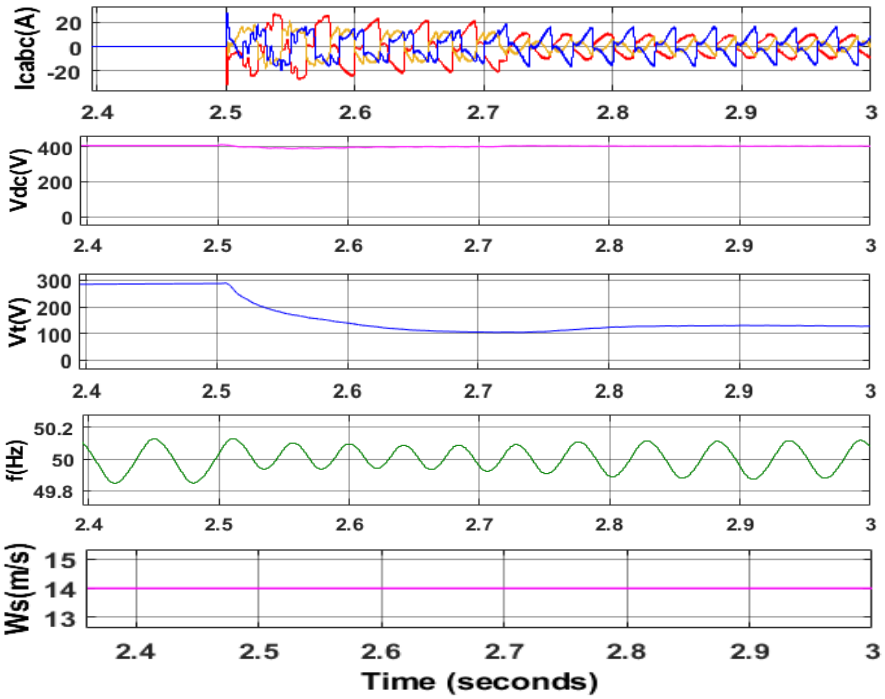

Figure 6: Waveforms of SEIG with constant wind speed and variable nonlinear load

4.3 Neutral current and Power balancing at variable nonlinear load.

Figure 7 illustrates, the source current in all three phases stays balanced and the neutral current from the supply side is zero. When the load from one phase is removed, there is a small frequency disruption, but the VCO-Free PLL reacts fast and tracks the reference frequency in a short amount of time. The generator, load, and battery system power measurements show that the power is balanced, with power flowing smoothly from the battery to the load or the other way around.

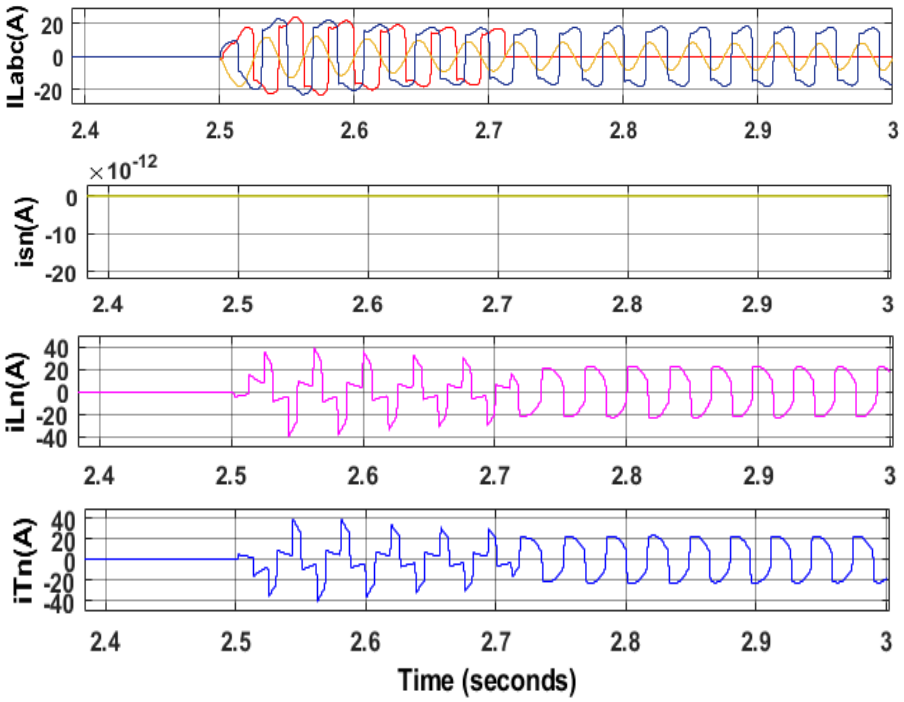

Industrial Engineering Journal
ISSN: 0970-2555
Volume : 53, Issue 12, No.2, December : 2024

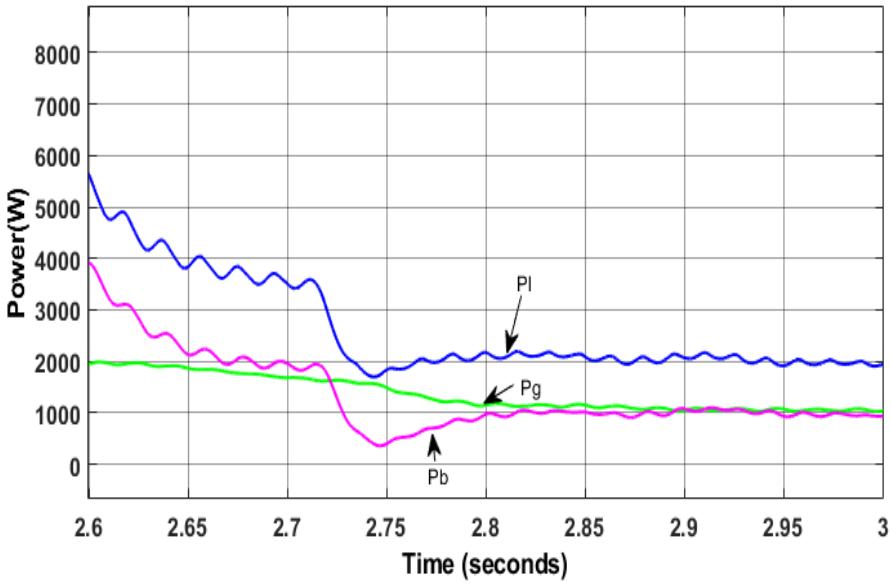

Figure 7: Compensation of Neutral current and Power with load transients

4.4 Transient response of SEIG with variable wind speed and variable load

Figure 8 depicts system under study is disturbed at two different moments, and the aforementioned parameters are observed, as shown in Figure 2(b). For thorough analysis, transients are introduced at two specific times: t=2.7 seconds and t=2.8 seconds. At t=2.7 seconds, the load on phase 'a' is disconnected, while at t=2.8 seconds, the wind speed (W_s) decreases from 14 m/s to 12 m/s. The key point of interest is the second instant, where wind speed decreases during a load unbalance. Despite the wind speed change, the magnitude of the PCI voltage remains constant, while the source current in all phases decreases following the decrease in wind speed. Since the load current remains unchanged, the additional supply current is directed toward the battery system via the VSI. As a result, the compensator current decreases after the second moment. This effect is also evident in the power flow of the generator, battery, and load, power supplied from the battery due to the less generation from the lesser wind speed. The behavior of other parameters remains consistent.

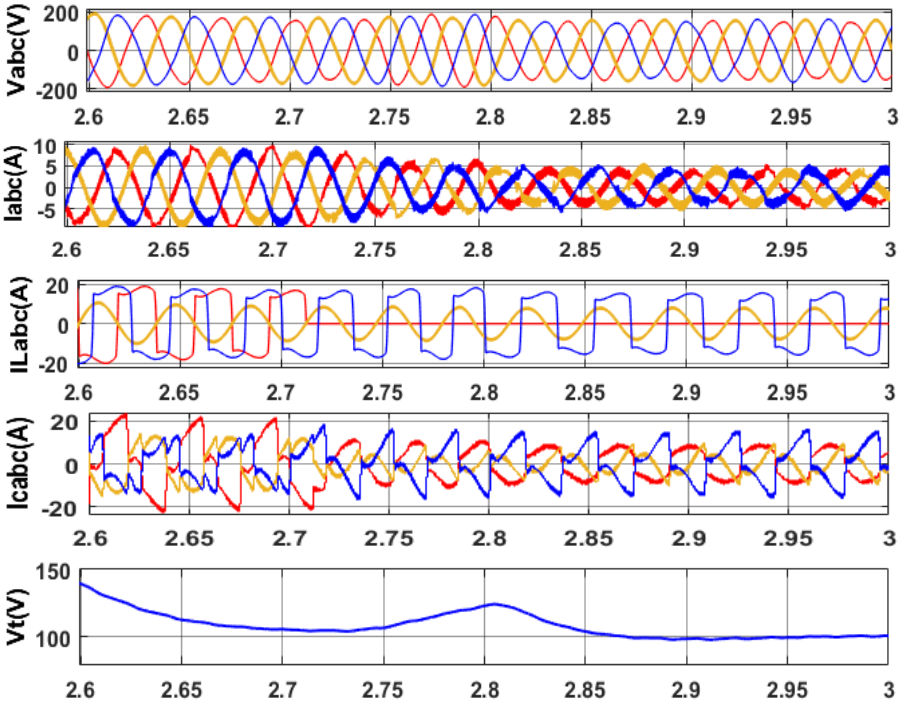

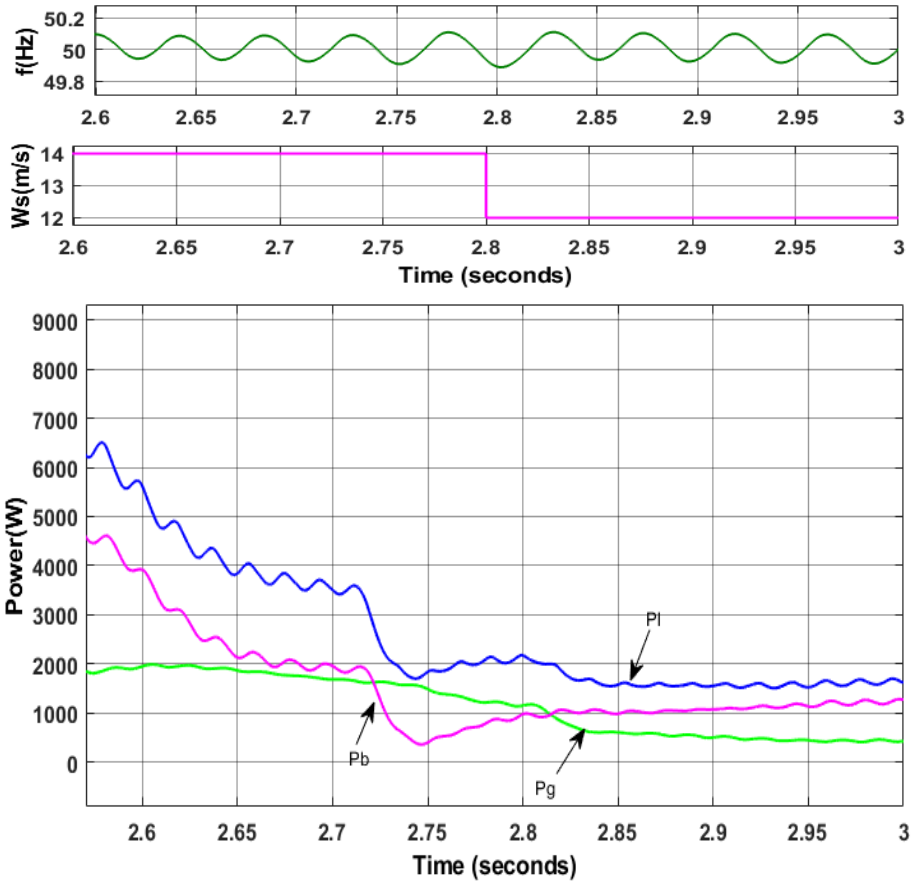

Figure 8: Waveforms of SEIG with variable wind speed and nonlinear load

V Conclusion

The VCO-free PLL control was implemented, and its performance was verified under varying load and wind conditions for improving power quality in the system studied. The system response with the developed control algorithm was found to be satisfactory. Voltage and frequency control objectives were achieved. The rationale for selecting the PLL without VCO is presented in detail. Unlike the SRF-PLL, which involves integrator and trigonometric function evaluation as part of the VCO, the VCO-free PLL avoids such complex calculations. Therefore, the response under transient conditions is superior compared to other PLLs that use a VCO. Additionally, a loop filter is not needed because there are no second harmonic fluctuations in the fundamental load current's calculated amplitude.
Scope of Future work is use an adaptive filters in loop filter of conventional SRF-PLL. Also Solar PV integration at DC link is necessary to maintain the power balance because the dump load is not a good option always balancing the power.

References

[1] Godoy Simoes, M., Farret, F.A(2008). 'Alternate energy systems, design and analysis with induction generators' (CRC Press, Taylor & Francis Group London, 2nd edn.) J. Clerk Maxwell, A Treatise on Electricity and Magnetism, 3rd ed., vol. 2. Oxford: Clarendon, 1892, pp.68–73.
[2]Lai, L.L., Chan, T.F(2007), 'Distributed generation: induction and permanent magnet generators' (John Wiley & Sons, Inc., England).
[3]Giri, A. K., Arya, S. R., & Vinnikov, D. Eds,(2022) : Distributed Energy Systems: Design, Modeling, and Control. CRC Press.
[4]Fox, B., Flynn, D(2007), 'Wind power integration connection and system operational aspects' (The Institution of Engineering and Technology, London, UK)

[5]Golestan, S., Guerrero, J.M., Vasquez, J.C(2017), 'Three-phase PLLs: a review of recent advances', IEEE Trans. Power Electron, 32, (3), pp. 1894–1907
[6]Gardner, F.M(2005), 'Phase lock techniques' (Wiley, Hoboken, NJ, USA, 3rd edn.)
[7]Karimi Ghartemani, M (2014), 'Enhanced phase-locked loop structures for power and energy applications' (Wiley-IEEE Press, Hoboken, New Jersey, USA)
[8]Chilipi, R.R., Singh, B., Murthy, S.S(2014), 'Performance of a self-excited induction generator with DSTATCOM-DTC drive-based voltage and frequency controller', IEEE Trans. Energy Convers, 29, (3), pp. 545– 557
[9]Rajagopal, V., Singh, B., Kasal, G.K(2011): 'Electronic load controller with power quality improvement of isolated induction generator for small hydro power generation', IET Renew. Power Generation, 5, (2), pp. 202–213
[10] Srikakolapu, J., Arya, S. R., Giri, A. K., Kundu, S., & Singh, M(2024),"DSTATCOM components modeling and control". Custom Power Devices for Efficient Distributed Energy Systems, pp. 21-42.
[11] Giri, A. K. K., Arya, S. R., Maurya, R., & Babu, B. C(2023)."Power quality improvement in stand-alone SEIG-based distributed generation system using Lorentzian norm adaptive filter". IEEE Transactions on Industry Applications,54(5), pp.5256-5266.
[12] Giri, A. K., Arya, S. R., Maurya, R., & Babu, B. C.(2019) : VCO-less PLL control-based voltage-source converter for power quality improvement in distributed generation system. IET Electric Power Applications, 13(8), pp.1114-1124
[13] Escobar, G.Ibarra, L., Valdez-Resendiz, J. E., Mayo-Maldonado, J. C), & Guillen, D(2021), Nonlinear stability analysis of the conventional SRF-PLL and enhanced SRF-EPLL. IEEE Access, 9, pp.59446-59455.
[14] S. Gude and C.-C. Chu(2019), ''Single-phase enhanced phase-locked loops based on multiple delayed signal cancellation filters for micro-grid applications,'' IEEE Trans. Ind. Appl., vol. 55, no. 6, pp. 7122–7133.
[15] H. Wu and X. Wang(2018,) ''Transient stability impact of the phase-locked loop on grid-connected voltage source converters,'' in Proc. Int. Power Electron. Conf. (IPEC-Niigata -ECCE Asia), pp. 2673–2680.
[16] H. Wu and X. Wang(2020) ''Design-oriented transient stability analysis of PLLsynchronized voltage-source converters,'' IEEE Trans. Power Electron., vol. 35, no. 4, pp. 3573–3589.
[17] Zamani, H., Karimi-Ghartemani, M., Mojiri, M(2018), 'Analysis of power system oscillations from PMU data using an EPLL-based approach', IEEE Trans. Instrum. Meas, 67, (2), pp. 307–316
[18] Gude, S., Chu, C.-C(2018), 'Dynamic performance improvement of multiple delayed signal cancelation filters based three-phase enhanced-PLL', IEEE Trans. Ind. Appl., 54, (5), pp. 5293–5305
[29] Giri, A. K., Arya, S. R., & Maurya, R. (2020), Transformer based Passive Neutral Current Compensation Techniques in Distributed Power Generation System. In First International Conference on Power, Control and Computing Technologies (ICPC2T) (pp. 379-384). IEEE.
[20] Golestan, S., Ebrahimzadeh, E., Wen, B., Guerrero, J. M., & Vasquez, J. C. (2020). dq-frame impedance modeling of three-phase grid-tied voltage source converters equipped with advanced PLLs. IEEE Transactions on Power Electronics, 36(3), 3524-3539.
[21] Jaklair, Lingappa, Guduri Yesuratnam, and Pannala Mallikarjuna Sarma(2020). "Control Algorithm for Renewable Energy Standalone System with Power Quality and Demand Management." Majlesi Journal of Electrical Engineering (2024).Volume18,Issue1,Pages 311-322, https://doi.org/10.30486/mjee.2024.2006726.1363